

Precipitation and temperature space–time variability and extremes in the Mediterranean region: evaluation of dynamical and statistical downscaling methods

Emmanouil Flaounas · Philippe Drobinski · Mathieu Vrac ·
Sophie Bastin · Cindy Lebeaupin-Brossier · Marc Stéfanon ·
Marco Borga · Jean-Christophe Calvet

Received: 24 February 2012 / Accepted: 3 October 2012
© Springer-Verlag Berlin Heidelberg 2012

Abstract This study evaluates how statistical and dynamical downscaling models as well as combined approach perform in retrieving the space–time variability of near-surface temperature and rainfall, as well as their extremes, over the whole Mediterranean region. The dynamical downscaling model used in this study is the Weather Research and Forecasting (WRF) model with varying land-surface models and resolutions (20 and 50 km) and the statistical tool is the Cumulative Distribution Function-transform (CDF-t). To achieve a spatially resolved downscaling over the Mediterranean basin, the European Climate Assessment and Dataset (ECA&D) gridded dataset is used for calibration and evaluation of the

downscaling models. In the frame of HyMeX and MED-CORDEX international programs, the downscaling is performed on ERA-I reanalysis over the 1989–2008 period. The results show that despite local calibration, CDF-t produces more accurate spatial variability of near-surface temperature and rainfall with respect to ECA&D than WRF which solves the three-dimensional equation of conservation. This first suggests that at 20–50 km resolutions, these three-dimensional processes only weakly contribute to the local value of temperature and precipitation with respect to local one-dimensional processes. Calibration of CDF-t at each individual grid point is thus sufficient to reproduce accurately the spatial pattern. A second explanation is the use of gridded data such as ECA&D which smoothes in part the horizontal variability after data interpolation and damps the added value of dynamical downscaling. This explains partly the absence of added-value of the 2-stage downscaling approach which combines statistical and dynamical downscaling models. The temporal variability of statistically downscaled temperature and rainfall is finally strongly driven by the temporal variability of its forcing (here ERA-Interim or WRF simulations). CDF-t is thus efficient as a bias correction tool but does not show any added-value regarding the time variability of the downscaled field. Finally, the quality of the reference observation dataset is a key issue. Comparison of CDF-t calibrated with ECA&D dataset and WRF simulations to local measurements from weather stations not assimilated in ECA&D, shows that the temporal variability of the downscaled data with respect to the local observations is closer to the local measurements than to ECA&D data. This highlights the strong added-value of dynamical downscaling which improves the temporal variability of the atmospheric dynamics with regard to the driving model. This article highlights the benefits and inconveniences

E. Flaounas (✉) · P. Drobinski · C. Lebeaupin-Brossier ·
M. Stéfanon
Laboratoire de Météorologie Dynamique, Institut Pierre Simon
Laplace, CNRS and Ecole Polytechnique, Palaiseau, France
e-mail: flaounas@lmd.polytechnique.fr

M. Vrac
Laboratoire des Sciences du Climat et de l'Environnement,
Institut Pierre Simon Laplace, CNRS and CEA, Saclay, France

S. Bastin
Laboratoire Atmosphères, Milieux, Observations Spatiales,
Institut Pierre Simon Laplace, CNRS and Ecole Polytechnique,
Palaiseau, France

C. Lebeaupin-Brossier
Unité de Mécanique, Ecole Nationale Supérieure des Techniques
Avancées-ParisTech, Palaiseau, France

M. Borga
Dipartimento Territorio e Sistemi Agro-Forestali,
University of Padova, 35020 Legnaro PD, Italy

J.-C. Calvet
CNRM/GAME, Météo-France and CNRS, Toulouse, France

emerging from the use of both downscaling techniques for climate research. Our goal is to contribute to the discussion on the use of downscaling tools to assess the impact of climate change on regional scales.

Keywords Mediterranean climate · Seasonal variability · Climate extremes · Downscaling · HyMeX · CORDEX · MED-CORDEX

1 Introduction

The Mediterranean basin is characterized by a nearly enclosed sea surrounded by very urbanized littorals and mountains, and is a sharp transitional zone between the semi-arid subtropics and mid-latitude regions. This climate is characterized by hot, long and dry summers, as also mild winters during which most rainfalls occur. Köppen (1936) defined the Mediterranean climate as one in which winter rainfall is more than three times the summer rainfall. Indeed, the seasonal variability of the Mediterranean climate is pronounced. Vautard et al. (2007) showed a direct connection between the rainfall and the temperature variability on an inter-annual cycle with generally hot summers preceded by anomalous dry winters generating severe droughts. Hot summers and droughts are linked through land surface/atmosphere feedbacks which play a key role in the seasonal variability of rainfall and temperature in the Mediterranean region with geographical specificities around the basin. They can have significant impact on public health, especially when combined with severe air pollution. A thoroughly studied example is the August 2003 heat wave which is considered to have caused thousands of deaths in France, Italy and Spain (e.g. Fischer et al. 2004; Garcia-Herrera et al. 2005). In addition to human risks, the prolonged droughts can result to great ecological disasters and often they might lead to extensive forest fires of great impact on air quality (Bussotti and Ferretti 1998; Pace et al. 2005).

The medium to high mountains that surround the Mediterranean Sea play a crucial role in steering the air flow and the Mediterranean Sea acts as a moisture and heat reservoir, so that energetic mesoscale atmospheric features can evolve to high-impact weather systems such as heavy precipitation during fall, cyclogenesis and wind storms during winter. Indeed, in winter the Mediterranean region is subject to stratospheric air intrusions in the lower troposphere, often resulting in extreme weather phenomena, (e.g. Lagouvardos and Kotroni 2000; Stohl et al. 2000; Zanis et al. 2003) such as storms and cyclones at times associated with extreme rainfall. The Mediterranean basin is known to present one of the highest concentrations of cyclones in the world, especially in winter (Pattersen 1956). However, the processes, the intensity and the concentration of cyclogenesis events

differ from area to area (Trigo Isabel et al. 1999), with the strongest events due to the interaction between the atmospheric flow and the orography (e.g. Atlas and Alps; Romero et al. 2000; Buzzi et al. 2003; Drobinski et al. 2001, 2005; Guénard et al. 2005). Among the environmental risks, extreme rainfall associated with floods is one of the greatest natural hazards in the region. For instance, in Spain 229 deaths by floods are reported between 1995 and 2004, due to cyclonic weather systems (Llasat-Botija et al. 2007).

The Mediterranean basin is identified as one of the two main hot-spots of climate change, meaning that its climate is especially responsive to global change (Giorgi 2006) with an increase in the interannual variability in addition to a strong warming and drying. Projections in anthropogenic scenarios show that global climate models converge and show evidence of a decrease of annual rainfall associated with an increase of heat-waves and droughts, expected to start earlier in the year and last longer, and an increase of rainfall variability (Giorgi 2006; Beniston et al. 2007; Giorgi and Lionello 2007).

Regional climate downscaling techniques are increasingly being utilized to produce regional climate information for impact and adaptation studies. It is thus critical that the potentials and limitations of regional climate downscaling-based information, along with the related uncertainties, are well understood by the modelling and user communities. It is a core objective of the World Climate Research Program (WCRP) endorsed programs CORDEX (COordinated Downscaling Experiment; Giorgi et al. 2009), MED-CORDEX (Ruti et al. 2012) and HyMeX (Hydrological cycle in the Mediterranean experiment; Drobinski et al. 2009a, b, 2010, 2011). Before downscaling global climate models (GCM) of anthropogenic scenario projections run in the framework of the 5th Climate Model Intercomparison Project (CMIP5) envisaged in the CORDEX, MED-CORDEX and HyMeX programs, a preliminary assessment of the performance of regional climate downscaling techniques has to be performed for the present climate with ERA-Interim (ERA-I) reanalysis (Uppala et al. 2008) of the European Centre for Medium-Range Weather Forecasts (ECMWF) as inputs.

In this article, dynamical and statistical downscaling (DD and SD, respectively) techniques are used. SD consists in obtaining high-resolution climate data from GCMs or reanalysis by deriving statistical relationships between observed small-scale variables (often station level) and larger scale variables (ERA-I), using either weather typing (e.g., Huth 2002; Vrac et al. 2007a; Boé and Terray 2008), regression models (through linear—e.g. Huth 2002; Wilby et al. 2002; Busuioc et al. 2008; Goubanova et al. 2010—or non-linear models—e.g. Sailor and Xiangshang 1999; Cannon and Whitfield 2002; Salameh et al. 2010; Vrac et al. 2007b; Ghosh and Mujumdar 2008), or stochastic weather generators (e.g., Semenov and Barrow 1997; Wilks and

Wilby 1999; Yang et al. 2005; Vrac and Naveau 2007; Vrac et al. 2007c; Carreau and Vrac 2011). Statistical downscaling may be used whenever suitable small-scale observed data are available to derive the statistical relationships. DD consists in driving a regional climate model (RCM) by a GCM over an area of interest since decreasing grid spacing generally improves the realism of the results (e.g., Mass et al. 2002; Sotillo et al. 2005; Déqué and Somot 2008; Ruti et al. 2008; Salameh et al. 2010; Herrmann et al. 2011).

Different inter-comparisons of downscaling techniques have been performed between DD models only (e.g. Frei et al. 2003, 2006; Déqué et al. 2008), between SD models only (e.g. Harpham and Wilby 2005; Lavaysse et al. 2012) or including both approaches (e.g. Busuioc et al. 2008; Brussolo et al. 2009; Quintana Seguí et al. 2010). However, in this latter category, the studies do not combine the two approaches but only compare the respective quality of the downscaled data (e.g. Haylock et al. 2008; Schmidli et al. 2006). Vrac et al. (2012) evaluated the respective performance of SD and DD and compare the potential the added-value of applying a SD model to different DD models over few local weather stations in Southern France. Generally, most of these inter-comparisons focused on one climate variable such as temperature (e.g. Spak et al. 2007) or precipitation (Schmidli et al. 2007) and, in general, evaluation or inter-comparison used data from local surface weather stations (e.g. Salameh et al. 2009; Lavaysse et al. 2012; Vrac et al. 2012). Regarding the specific use of gridded data for SD, it has been restricted to monthly climatologies (e.g. CRU; see Mitchell and Jones 2005) filtering a significant part of the space–time variability of near surface temperature and precipitation, thus preventing any investigation of climate extremes.

Key issues are thus still open regarding joint SD and DD assessment. Most SD models are calibrated on local weather stations, even though on-going research aims at modelling the space-dependence of local weather stations to improve SD (Vrac et al. 2007d). Therefore, most SD techniques do not integrate spatial variability information, so DD technique should be more appropriate to reproduce the fine scale spatial pattern of climate information (e.g. given by near-surface temperature and precipitation). In Vrac et al. (2012), the combined use of SD and DD models improved the spatial pattern of near-surface temperature, precipitation and wind speed with respect to SD only, suggesting the added-value of using DD technique to provide the fine scale spatial variability to the locally calibrated DD technique. However, this study only used few surface weather stations located in Southern France. To challenge this conclusion, the use of gridded data at high space–time resolution is relevant.

In this article, we thus use the European daily gridded dataset of temperature and precipitation from the European Climate Assessment and Dataset (ECA&D) project (Haylock et al. 2008). The fine spatial resolution ($0.25^\circ \times 0.25^\circ$ in longitude and latitude) and high frequency (daily averages) allows to compare SD and DD over a domain with a horizontal resolution similar to that of DD grid (i.e., 20–50 km resolution). Using the ECA&D database at high temporal resolution, we can also assess in depth the respective ability of SD and DD models and joint SD/DD approach to:

- retrieve accurately the spatial fine scale pattern of temperature and rainfall
- retrieve accurately the time variability of temperature and rainfall
- reproduces climate extremes (cold and warm extremes, extreme precipitations).

This study addresses these issues at the whole Mediterranean basin scale but also focuses on sub-regions with specific climate specificities (arid regions, coastal regions and mountainous regions). In this paper, we address these issues using the Weather Research and Forecasting (WRF) model (Skamarock and Klemp 2008) as the DD model and the Cumulative Distribution Function-transform (CDF-t) as SD tool (Michelangeli et al. 2009). We investigate the impact of WRF configuration, by performing simulations with two different land surface models and two different horizontal resolutions (20 and 50 km). Land surface models basically compute the surface fluxes (sensible and latent heat fluxes and ground flux) which control partly precipitation triggering, and from which near surface temperature is derived. Increasing horizontal resolution is expected to improve WRF skills by producing detailed information on land-use and topography and by improving the representation of the fine scale features of the atmospheric circulation. The four WRF integrations provide an ensemble of simulations on which CDF-t is applied in a SD/DD approach. This ensemble of downscaled temperature and precipitation allows to quantify the uncertainty associated with downscaling.

In the following, Sect. 2 describes the DD and SD techniques, the observations and the methodology used in this study. Section 3 introduces the seasonal, the extremes and the intraseasonal variability of near surface temperature and rainfall in the Mediterranean region, as observed by the gridded observations of ECA&D. Section 4 quantifies the ability of DD, SD and SD/DD combined approach to reproduce the space–time variability of temperature and precipitation, as well as their extremes. Section 5 discusses the added-value of each technique with respect to the other and concludes the study with suggestions for future work.

2 Downscaling techniques, observations and methodology

As part of phase I of MED-CORDEX and HyMeX, the large-scale driving fields provided as input for statistical downscaling (SD) and as initial and boundary conditions for dynamical downscaling (DD) are the 6-hourly meteorological fields from the ERA-I reanalysis which has a $0.75^\circ \times 0.75^\circ$ horizontal resolution in longitude and latitude, available since the year 1979 (Dee and Uppala 2009).

2.1 Dynamical downscaling (DD)

The model used to downscale ERA-I in the framework of MED-CORDEX and HyMeX is the version 3.1.1 of the Weather Research and Forecasting Model (WRF). WRF is a limited area model, non-hydrostatic, with terrain following eta-coordinate mesoscale modeling system designed to serve both operational forecasting and atmospheric research needs (Klemp et al. 2007; Skamarock and Klemp 2008). We use the physical options chosen to perform the HyMeX/MED-CORDEX simulations (Lebeau-pin Brossier et al. 2011, 2012a, b, c). These include the WRF Single-Moment 5-class microphysical parameterization (Hong et al. 1998, 2004), the new Kain-Fritsch convective parameterization (Kain 2004), the Dudhia shortwave radiation (Dudhia 1989) and Rapid Radiative Transfer Model longwave radiation (Mlawer et al. 1997) and the Yonsei University planetary boundary layer scheme (Noh et al. 2003). Two land surface models (LSM) have been used in this study, namely the Rapid Update Cycle (RUC) LSM and the thermal diffusion (DIF) LSM (detailed hereafter). In the context of HyMeX/MED-CORDEX, ocean/atmosphere coupled simulations have also been performed using WRF with such configuration (Drobinski et al. 2012; Claud et al. 2012; Lebeau-pin Brossier et al. 2012c).

Initial conditions are provided for January 1st, 1989 and the time interval for the boundary conditions is 6 h. In the vertical, 28 unevenly spaced levels are used and the atmosphere top is at 50 hPa (sensitivity tests have been performed with more vertical levels without significant differences; 28 levels is the optimal choice for climate simulations with regards to both for CPU time and data storage). The sea surface temperature is provided by ERA-I. The geographical data are from 5 minutes resolution United States Geophysical Survey data. Soil type is based on a combination of the 10-min 17-category United Nations Food and Agriculture Organization soil data and U.S. State Soil Geographic 10-min soil data. A complete set of physics parameterizations is used Kain and Fritsch for the cumulus parameterization (Kain 2004); the YSU PBL scheme (Hong and Pan 1996); RRTMG for the longwave and shortwave radiation schemes (Mlawer et al. 1997).

Two land surface models (LSM) have been used in this study, namely the Rapid Update Cycle (RUC) LSM and the thermal diffusion (DIF) LSM. The RUC LSM (Smirnova et al. 1997) resolves heat and moisture transfer in 6 layers from 0 to 3 m. This scheme accounts for the different phases of soil surface water, vegetation effects (evaporation from leaf stomata, solar radiation absorption, heat fluxes etc.) and canopy water. Initial conditions are required for soil temperature and moisture. The DIF LSM is based on a 5-layer simple LSM where the energy budget includes radiation, sensible and latent heat. The last layer goes as deep as 16 cm, under which an average of temperature is applied. Vegetation effects are not taken into account and initial conditions are not required. The initial soil moisture is fixed to a constant value which is a function of the land use and the season. During the simulation, an empirical coefficient, called soil moisture availability which is a function of the land use and the season, is applied for latent heat flux calculation. More details on the schemes can be found in Skamarock et al. (2008). The WRF simulation has been relaxed towards the ERA-I large scale fields with a nudging time of 6 h (Salameh et al. 2010). Four WRF simulations have been performed over the ERA-I period, from 1989 to 2008 (recently made available 1979 onwards). Two simulations have been performed with a horizontal resolution of 50 km with RUC (hereafter referred as WRF/RUC 50) and DIF (hereafter referred as WRF/DIF 50) LSM and two have been performed with a horizontal resolution of 20 km, also with RUC (hereafter referred as WRF/RUC 20) and DIF (hereafter referred as WRF/DIF 20) LSM.

2.2 Statistical downscaling (SD)

The statistical downscaling used in this study is the “Cumulative Distribution Function-transform” (CDF-t) method developed by Michelangeli et al. (2009) which was first applied by Oettli et al. (2011), Lavaysse et al. (2012) and Vrac et al. (2012) for the downscaling of variables such as wind, temperature and precipitation. This approach aims at relating the cumulative distribution function (CDF) of a climate variable (e.g., wind) at a large scale (i.e. here from ERA-I reanalysis or WRF simulations) to the CDF of this variable at a local scale (i.e. at a grid point of the ECA&D gridded dataset). CDF-t can be seen as a variant of the quantile–quantile correction method (e.g., Déqué 2007) that can use either non-parametric (as in Déqué 2007) or parametric (as in Piani et al. 2010) correspondences between predictors and predictands quantiles in order to derive local scale CDFs (i.e., at the stations) based on the evolutions of the large-scale CDFs between calibration and evaluation period. Although the CDF-t and quantile–quantile methods have a similar objective, CDF-t takes into account the change in the large-scale CDF from the

calibration to the evaluation period, while quantile–quantile projects the simulated large-scale values onto the historical CDF to compute and match quantiles. In the CDF-t approach, a mathematical transformation T is applied to the large-scale CDF to define a new CDF as close as possible to the CDF measured at the station.

Let F_{Lc} and F_{lc} define respectively the CDFs of a given variable from ERA-I reanalysis or WRF simulations and from the local observations, both for the calibration period (L and l indices stand for large-scale and local-scale, respectively; c index stand for calibration period), then the transformation T is defined as follows:

$$T(F_{Lc}(x)) = F_{lc}(x), \text{ for all } x \text{ in the domain of the variable.} \quad (1)$$

Replacing x by $F_{Lc}^{-1}(u)$, where u belongs to $[0, 1]$ we obtain a representation for T :

$$T(u) = F_{lc}(F_{Lc}^{-1}(u)) \quad (2)$$

Assuming that the validity of the transformation T stands for the evaluation period (or any future projection or short-term forecasts), then given the CDF F_{Le} calculated from the large-scale fields provided by WRF or ERA-I over the evaluation period (index e stands for evaluation period), the CDF-t model will provide the local CDF as follows:

$$F_{le}(x) = T(F_{Le}(x)) \quad (3)$$

or equivalently,

$$F_{le}(x) = F_{lc}(F_{Lc}^{-1}(F_{Le}(x))), \quad (4)$$

for any x in the domain of the variable.

For instance, to run the CDF-t model for an application of local future climate projections one may use the time series of historical observations of a variable from a meteorological station and the same variable from a large-scale model, interpolated to the location of the station. Then, for a given past-to-present period (*calibration period*) the CDF-t model will adapt the mathematical relation between the CDF of the model and the CDF of the observations. Finally, this relation will be applied to the model interpolated values of future projections. Based on the CDF F_{le} determined by CDF-t, the generation of local-scale values is then performed by applying the quantile–quantile method between F_{le} and F_{Le} (and not between F_{lc} and F_{Lc} as in the “classical” quantile–quantile approach). In order to perform an effective downscaling with the CDF-t model, there is one main assumption: the mathematical relation generated by the CDF-t model is temporally stable.

It is important to note that the CDF-t has been calibrated without distinction between the seasons. Indeed, the ECA&D gridded dataset used to calibrate CDF-t (see Sect. 2.3) provides daily averages on a 25 km resolution grid affected by some spatial smoothing due to the interpolation

procedure. Tests have shown that for such dataset as a reference, the uncertainty associated with CDF-t increases significantly when performing seasonal distinction (the number of data used for calibration is divided by 4) without beneficial effect of consideration the seasonality of the extremes due to rather smoothed spatial and temporal variability of the extremes.

2.3 Observations

The downscaled variables are the distributions of the daily near-surface temperature and precipitation. To calibrate the SD model and evaluate the downscaled distributions from SD and DD techniques, we make use of the European daily gridded dataset of temperature and precipitation from the ECA&D project (Klein Tank et al. 2002; Haylock et al. 2008). The ECA&D project integrates data from 57 participants for 62 countries, which correspond to 26,061 series of observations for 12 elements at 4,823 meteorological stations throughout Europe and the Mediterranean area. The gridded dataset is produced with a horizontal resolution of $0.25^\circ \times 0.25^\circ$ in longitude and latitude. Its accuracy depends on the density of the surface weather stations which is zero over sea and weak over mountainous regions. Here only the common period between ERA-I and ECA&D is used, i.e. 1989–2008.

The ECA&D daily rainfall and temperature dataset has been evaluated over the Mediterranean region by comparing its field values with station observations (Flaounas et al. 2012a). The ECA&D dataset tends to underestimate the rainfall extremes while for temperature it shows rather small biases depending on the region. It has been shown that the performance of ECA&D depends on the spatial density of the included station observations. For instance, Flaounas et al. (2012a) showed that two stations located in Southern France and not “assimilated” within ECA&D, one in the mountains and one near the Mediterranean coast present very different rainfall intra-seasonal variability despite their proximity (about 50 km). Due to the low density of the observations included in the ECA&D in this region, the ECA&D dataset attributes, unrealistically, very similar variability patterns to the two stations.

2.4 Methodology

The near-surface temperature (temperature at 2 m) and precipitation fields from the four WRF simulations and the ERA-I reanalysis are bi-linearly interpolated to the ECA&D grid points.

Since the WRF model is forced by ERA-I reanalysis over the period 1989–2008, we split the dataset in two periods for SD calibration and evaluation: the *calibration period* extends between 1989 and 1998 and the *evaluation period*

between 1999 and 2008. The evaluation of SD models is a challenging task. Ideally, the best we could do is to calibrate SD models over a given time period and evaluate them on another time period with climate conditions very different from those of the calibration period. As we do not dispose of reliable observed data for a climate very different from the one used for calibration, the least that we can (should) do is to cut into two parts the time series that we have at our disposal. We also split the time series in two randomly without any different results. At least, this allows to evaluate the SDMs on data that were not used during the calibration process. In other words, although the calibration periods (only 10-year time period) may not cover the “climatology” in the region, we hope that they contain sufficiently varied situations to capture the main relationships between large and local-scale data within the calibrated SD model to be applied in another climate context. The calibration period is used here to derive the transform functions T of CDF-t relating the four WRF simulations and the ERA-I reanalysis with ECA&D time series at each grid point. The calibration is performed without distinction between the seasons. The transform functions are used to produce downscaled CDF of near-surface temperature and precipitation over the evaluation period. The downscaled values are then compared to the observations.

Specific processing needs to be applied to the precipitation data since zero rainfall values create a singularity in the precipitation distribution which can hardly be modeled by SD. It is also well known that numerical models produce too many low precipitation events. In the following, daily rainfall below 1 mm in WRF simulations, ERA-I reanalysis and ECA&D dataset (due to the interpolation of station observations on a regular grid) are put to zero (non precipitating day). This is a commonly used approach.

In the following, the assessment of the regional climate downscaling techniques (WRF and CDF-t) is performed with respect to the ECA&D observations over the evaluation period (1999–2008) for summer (June to August) and winter (December to February). Different metrics are used for this assessment. The 50th quantile is used as an indicator of the “median” climate, while the 5th and 95th temperature quantiles and the 95th rainfall quantile to investigate climate extremes (e.g. Frei et al. 2006).

The similarity between the ECA&D data and the corresponding field from ERA-I and downscaling methods (SD, DD and SD/DD) is quantified with maps of bias allowing a regional “view” of the models deficiencies and advantages. It is also quantified in terms of their correlation, centered root-mean square difference and standard deviation plotted in Taylor diagrams. A “zoom” over five sub-regions with different “climates” and various terrain complexities is also provided. These regions are illustrated in Fig. 1. They are the Middle East, the western Mediterranean, the eastern

Mediterranean, the northwest Africa and the Alps. Middle East and North Africa are arid regions, whereas western and eastern Mediterranean are more influence by mid-latitude climate. The Alpine region is investigated separately since it is the highest mountain ridge of the Mediterranean basin.

3 The Mediterranean climate from ECA&D dataset

Figure 2 shows the ECA&D values of the 5th, 50th and 95th quantile of near-surface temperature for winters and summers of the period 1999–2008 (evaluation period). In winter, the western and eastern Mediterranean sub-regions (Fig. 1) present temperatures between -10 and 15 °C with a median of about 10 °C. The coldest values are observed in the Alps with cold extremes below -20 °C and the warmest temperatures are observed in Middle East and North Africa with warm extremes above 20 °C. In summer, temperatures over the whole Mediterranean region increase by 15 – 20 °C with respect to winter values. The lowest values are observed over the Alps (cold extremes are about 0 °C) and the warmest in North Africa (warm extremes exceed 40 °C).

Figure 3 displays the patterns of the 50th and 95th rainfall quantiles from the ECA&D observations. In winter, maximum rainfall is mainly observed over the mountainous regions surrounding the Mediterranean Sea due to forced orographic lifting of moist air advected by strong marine low-level jets (e.g. Lebeaupin Brossier et al. 2006; Ducrocq et al. 2008, 2012a, b, c). In summer, strong precipitation are frequent in the European continental plains due to thermal convection and along the slope of the major mountain ridges (e.g. Alps) due to alpine pumping (e.g. Raymond and Wilkening 1980; Weissmann et al. 2005).

4 Downscaled near-surface temperature and rainfall

4.1 Spatial variability and extremes

Figures 4 and 5 show the temperature bias between the downscaling methods and the observations for the seasonal 5th, 50th and 95th quantiles for winter and summer, respectively. The upper rows of Figs. 2a and 3a present the temperature bias for ERA-I. The bias is weak ranging between -1 and 1 °C in winter and summer. However, in summer, a significant warm bias exceeding 3 °C, is observed over the mountainous regions and Middle East. During summers the strong local forcing in anti-cyclonic conditions, combined with less dense observation network, impacts the quality of the retrieved temperature field. Concerning the temperature extremes, ERA-I performs equally well for both warm and cold extremes with at most 2 – 3 °C absolute bias over very few small areas. The fairly

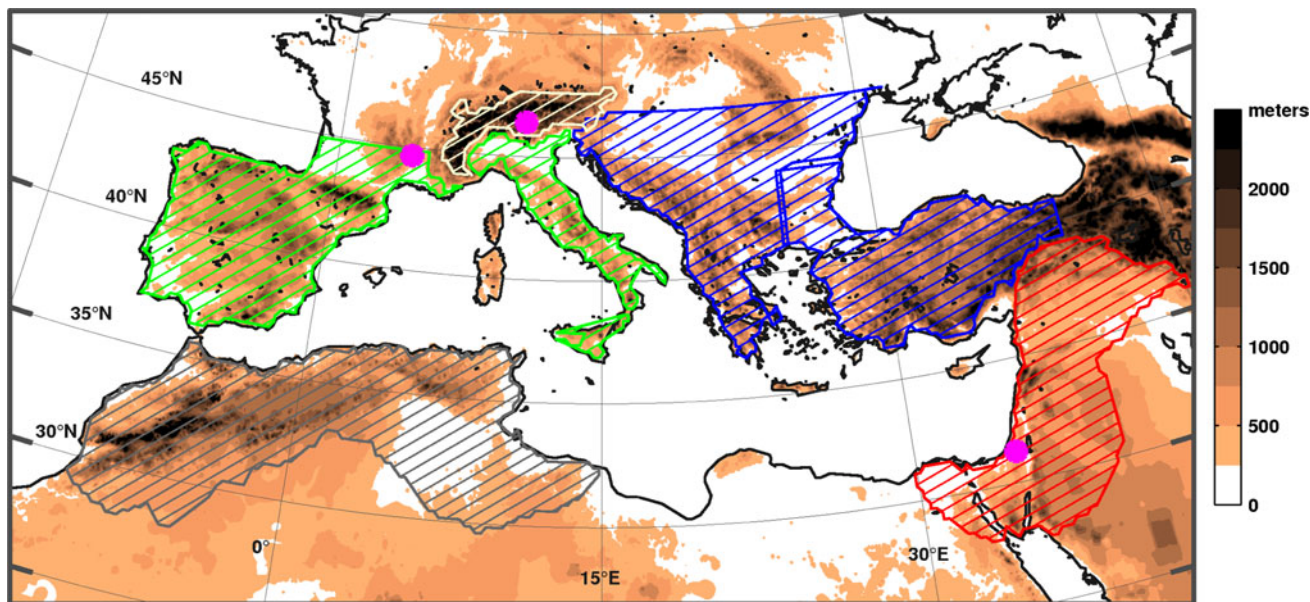


Fig. 1 The WRF simulation domain and its orography. *Hatched areas* illustrate the different regions taken under consideration for the Taylor diagrams and for the wet and dry spells table: Middle East in *red*, east Mediterranean in *blue*, west Mediterranean in *green*, Alps in *yellow* and North Africa in *gray*. *Dots in magenta* represent the locations of observation stations

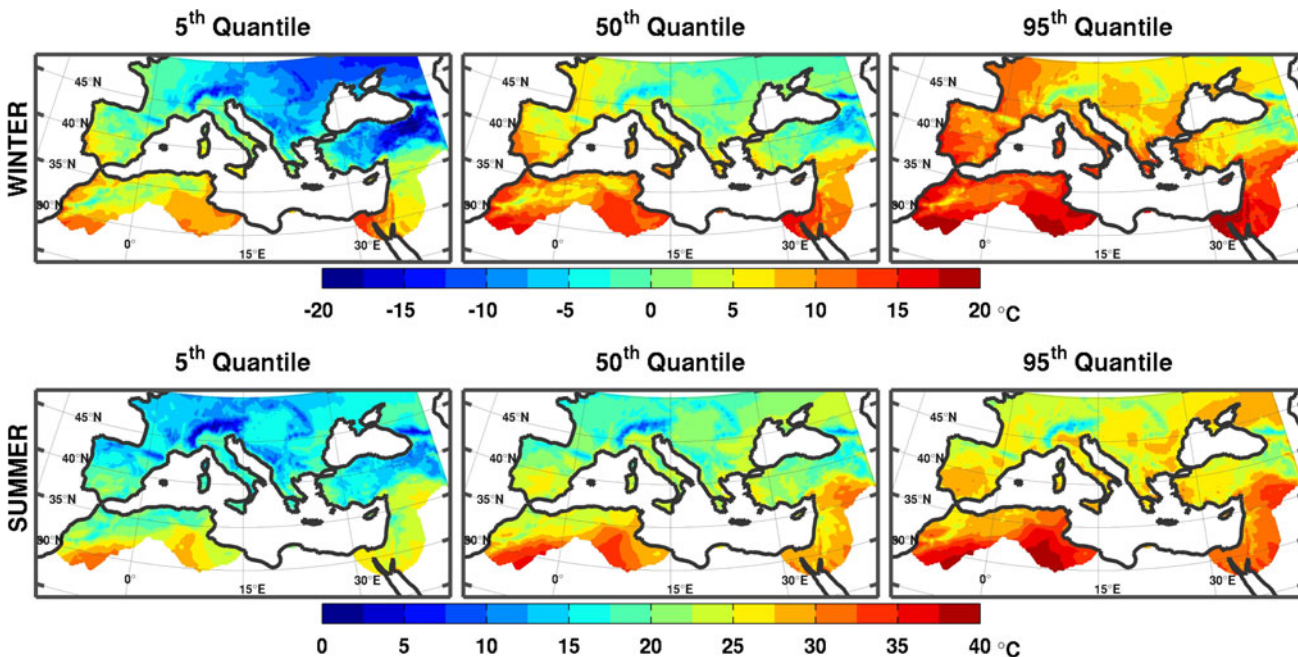


Fig. 2 The 5th (*left column*), 50th (*middle column*) and 95th (*right column*) quantiles of the 2-m temperature for winter (December to February; *upper row*) and summer (June to August; *lower row*) over

1999–2008, for the ECA&D. Note that the *color axis* differs for winter and summer (shift by +20 °C)

good performance of the ERA-I reanalysis is expected since many ECA&D surface stations are assimilated within the ECMWF assimilation system. Conversely, DD with WRF displays larger seasonal bias. Figures 4 and 5 show significant bias over the whole domain. The temperature pattern from DD is thus worse than that from ERA-I reanalysis which is used to drive DD model WRF. In

winter, the WRF/RUC simulations have a warm bias of approximately 2 °C for the median and both cold and warm extremes, while the WRF/DIF simulations underestimate the cold extremes with a significant warm bias of more than 4 °C in Eastern Europe (Fig. 4a). In summer, WRF simulations are extremely sensitive to the LSM (Fig. 5a; 2nd to 5th rows). The use of RUC LSM produces an almost

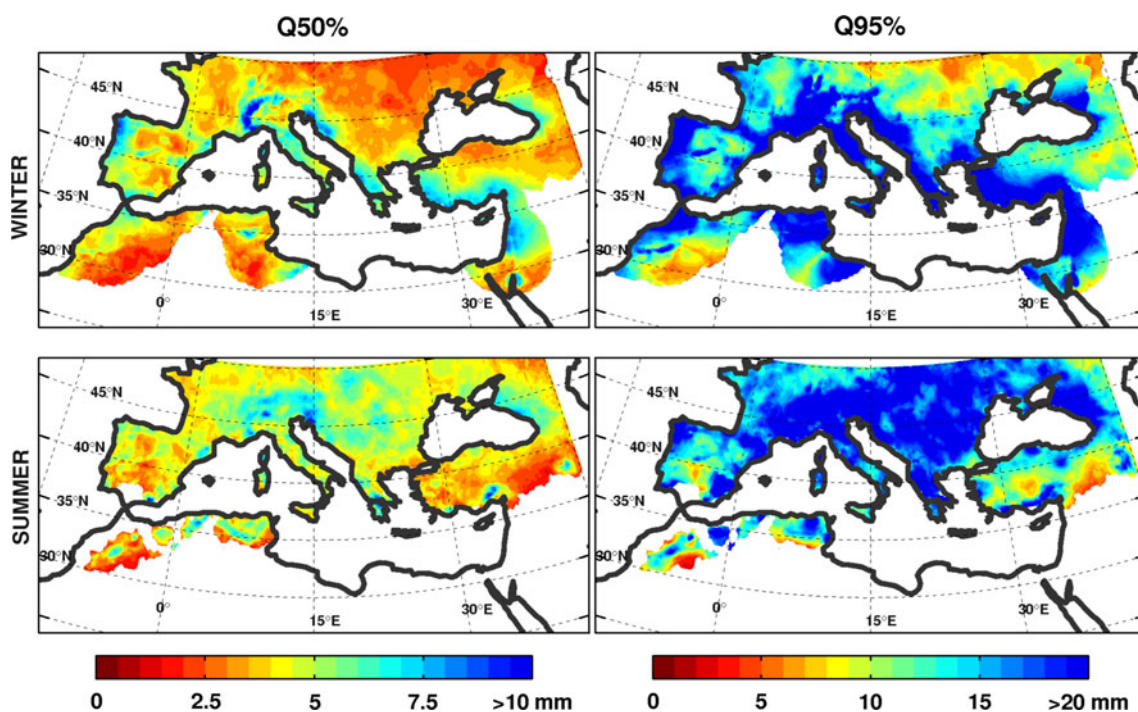


Fig. 3 The 50th (left column) and 95th (middle column) quantiles of daily rainfall from ECA&D observations for winter (December to February) (upper row) and summer (June to August) (lower row) over 1999–2008. The right column displays to number of rainy days

(i.e. positive rainfall) for winter (upper row) and summer (lower row) from ECA&D observations over 1999–2008. Note that the color axis differs for Q50 % and Q95 % (shift by +10 mm)

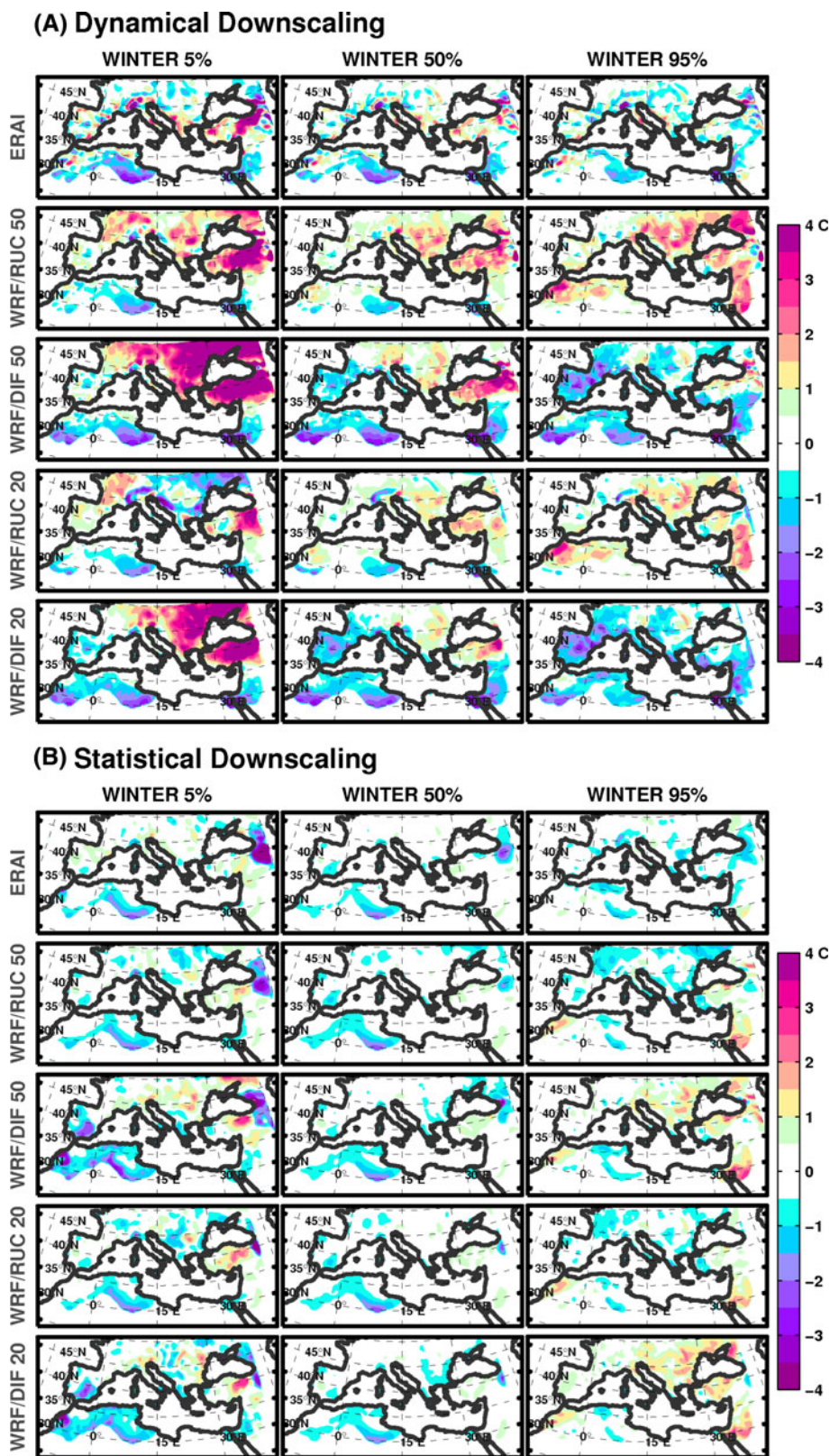
homogeneous warm bias of approximately 3–4 °C over the whole domain, whereas the use of DIF LSM produces a cold bias exceeding -4 °C everywhere. Part of the WRF/DIF cold bias is attributed to the soil moisture availability which is constant with time and has been set to its winter climatological value. Such simple LSM is not adapted to regions where summertime soil water scarcity is frequent in summer and thus sensible heat flux is considerably underestimated in these simulations. One can note that the finer resolution, the lower the near-surface temperature. This increases the cold bias (in absolute value) and reduces the warm bias where they exist in the simulations performed with a 50 km resolution grid. The use of SD with CDF-t plugged into WRF simulations and ERA-I reanalysis, performs significantly better than DD with WRF. The absolute bias for both winter and summer is lower than 1 °C (Figs. 4b, 5b). Despite the opposite temperature bias of WRF/DIF and WRF/RUC, a 2-stage downscaling chain, with CDF-t applied to the WRF simulations seems to correct the biases produced by WRF only. Such 2-stage approach applied on specific weather stations in Vrac et al. (2012) did not systematically improve the downscaled temperature.

Figure 6 displays the Taylor diagram for the seasonal mean and extremes of near-surface temperature with respect to ECA&D, for the five sub-regions shown in Fig. 1. For all regions, ERA-I as well as DD and SD

perform well with in general correlation exceeding 0.8 and standard deviation at worst 20 % lower than in ECA&D. The results are also very similar whatever the quantile. In detail, ERA-I is at best performing as good as DD with similar correlation and standard deviation but in most cases, displays slightly lower performance. SD is always closer to the ECA&D data. The effect of the horizontal resolution and land surface model is not so clear for temperature downscaling, except for the Alps. In the Alps, a finer horizontal resolution improves the spatial correlation of the downscaled temperature field with respect to the ECA&D. The effect on standard deviation is however not systematically beneficial. Regarding the added-value of combined SD/DD approach, it is non significant for temperature. Using CDF-t to downscale ERA-I reanalysis or WRF simulations does not produce different skills for spatial correlation and variability. Regarding the bias displayed in Figs. 4b and 5b, this still holds when RUC land surface model is used. Conversely, using CDF-t with WRF/DIF even degrades the bias with respect to CDF-t/ERA-I.

Regarding rainfall, Fig. 7 shows the relative bias of downscaled rainfall and rainfall from ERA-I with respect to ECA&D rainfall shown in Fig. 3. Figure 7a shows that ERA-I reanalysis and all WRF simulations (i.e. DD) display very similar spatial patterns with DD presenting systematically stronger bias regardless the season and quantile. During winter, DD produces better downscaled

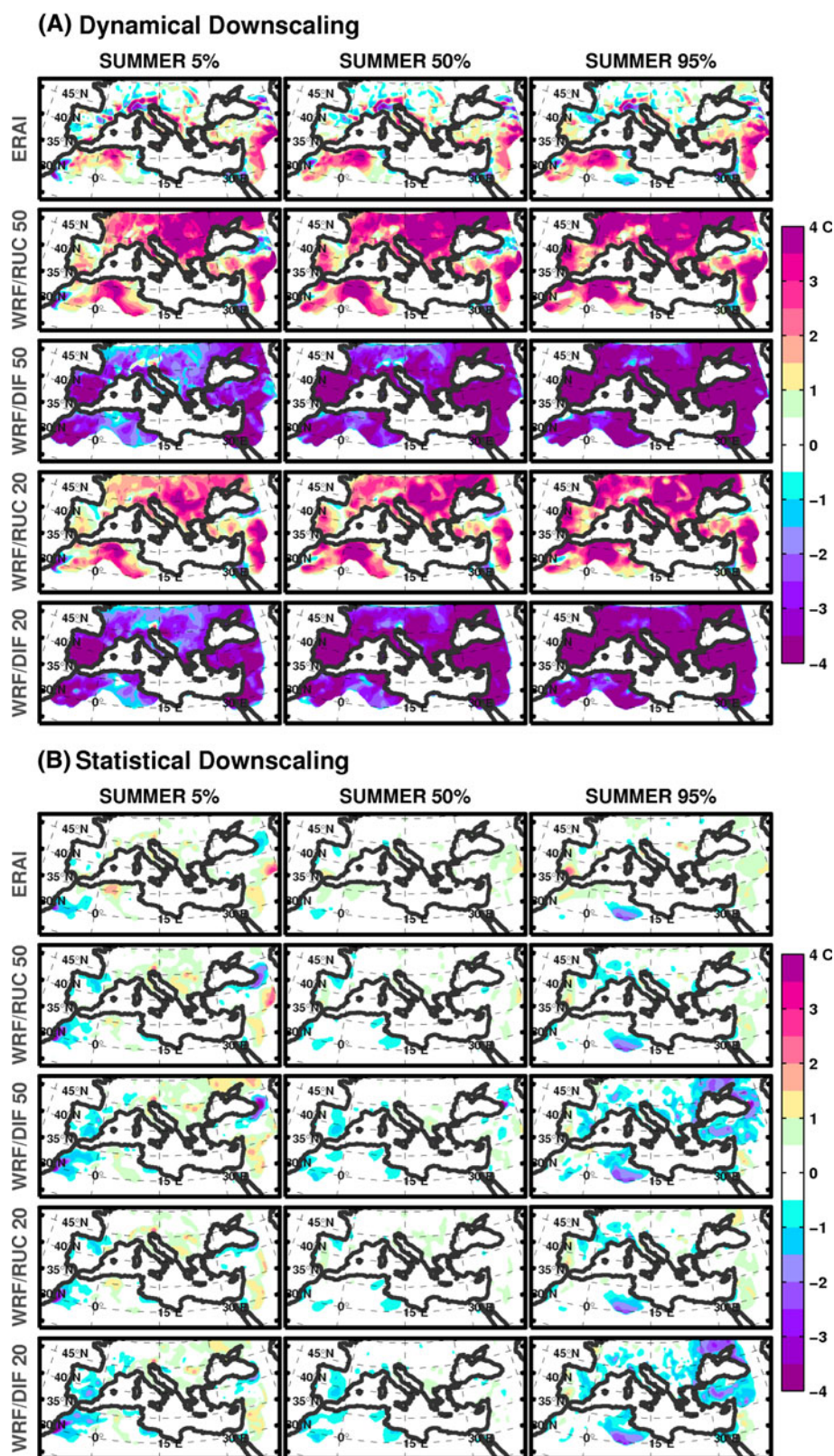
Fig. 4 **a** Difference between the downscaled and observed 5th quantiles (*left column*), 50th quantiles (*middle column*) and 95th quantiles (*right column*) for the 2-m temperature in winter for dynamical downscaling over 1999–2008 (evaluation period) for ERA-I reanalysis (*1st row*), WRF/RUC 50 simulation (*2nd row*), WRF/DIF 50 simulation (*3rd row*), WRF/RUC 20 simulation (*4th row*) and WRF/DIF 20 simulation (*5th row*); **b** same as panel a but for statistical downscaling



rainfall over the Western Mediterranean where it never exceeds -50% , than over the Eastern Mediterranean where it exceeds $+50\%$. However, comparing the relative bias to

ECA&D rainfall in Fig. 3, 50% relative bias corresponds to about 1 mm daily rainfall bias. Regarding extremes, DD overestimates rainfall by 50% and more all over the

Fig. 5 Same as Fig. 4 but for summer



domain except in Middle East where rainfall is underestimated by about -50% . In summer, ERA-I and DD show low bias ranging between -20 and 20% (i.e. less than

0.4 mm in absolute value). The similar performance of all WRF simulations could be attributed to the use of the same cumulus and planetary boundary layer parameterizations.

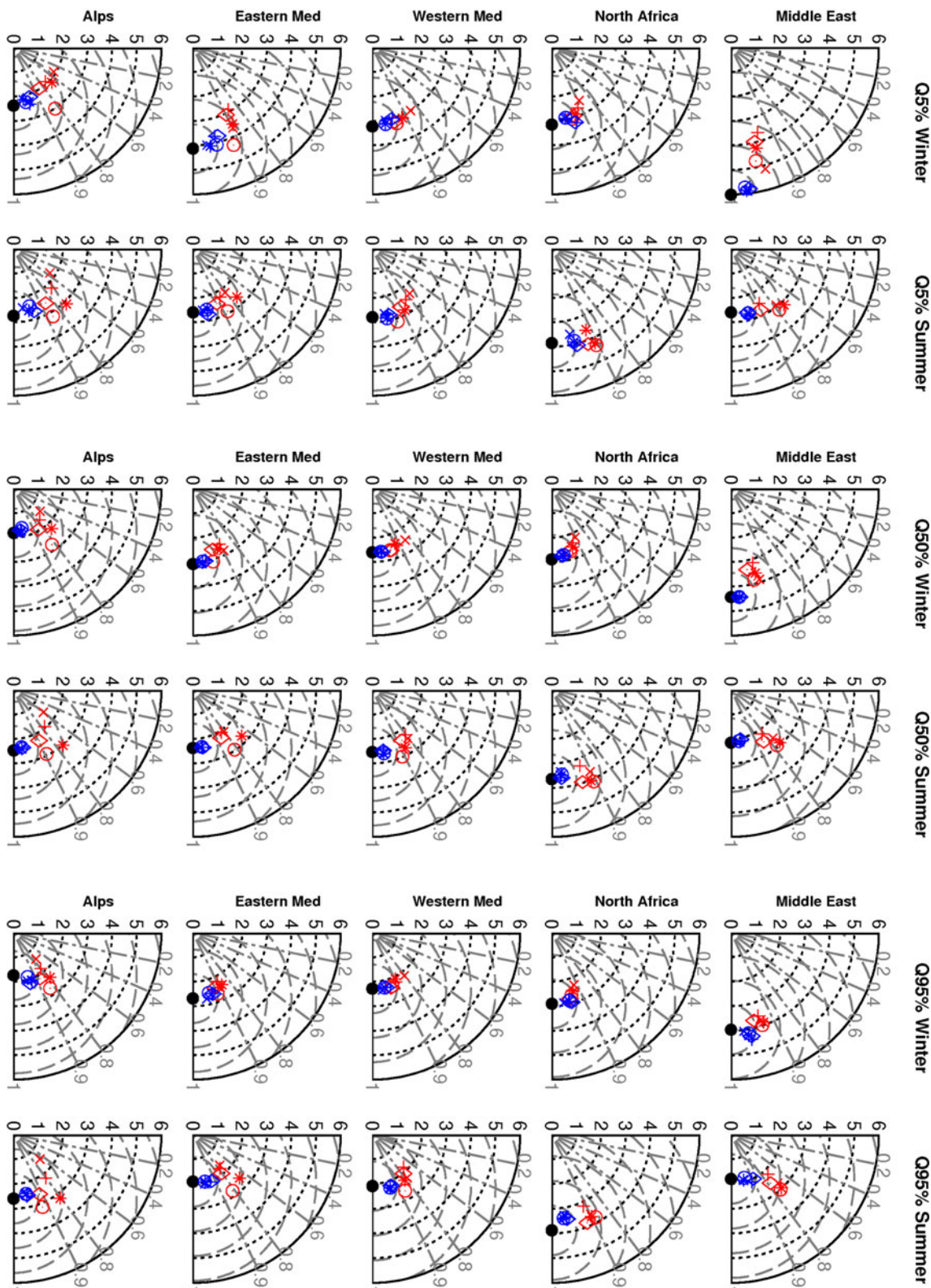


Fig. 6 Taylor diagrams for winter and summer temperature median and extremes (q5obs, q50obs and q95obs), for ERA-I, DD, SD and SD/DD, regards to ECA&D in the five sub-regions illustrated in Fig. 1. Root mean square differences in all figures are plotted with

1 °C of interval. Symbols in red stand for DD and ERA-I, while in blue for CDF-t. Black dot stands for the ECA&D, X for ERA-I; star for WRF/RUC50; circle for WRF/DIF50; cross for WRF/RUC20 and the diamond for WRF/DIF20

The two parameterizations control temperature and humidity distribution within the whole atmospheric column, and rainfall triggering. The Mediterranean domain is also sufficiently small to produce strong control of the simulations by the boundary conditions (Omran et al. 2012), which prevents significant departure from the driving large-scale field. It plays a similar role as nudging which is also applied in these simulations in the free troposphere only as suggested by Lo et al. (2008). Overall, it has been shown that such a relaxation to the large-scale driving fields is rather beneficial to the WRF rainfall outputs, compared to the observations (Lo et al. 2008). Figure 7b shows the results for SD. The 50th rainfall quantile has a relative bias ranging between 20 and 40 % in winter and less than -30 % in summer. Comparing SD and DD, one can first note that even with strong bias in ERA-I reanalysis and WRF simulations (between -50 and -100 %), SD provides an a posteriori correction with results similar whatever the quality of the inputs.

Figure 8 shows the Taylor diagrams for the seasonal mean and extremes of rainfall with respect to ECA&D, for the five sub-regions shown in Fig. 1. The effect of the horizontal resolution of the DD model is much more striking for precipitation than for temperature whatever the rainfall quantile. Higher resolution systematically increases rainfall standard deviation. It is particularly visible during winter. However, counter-intuitively higher resolution does not improve significantly the spatial correlation of the rainfall pattern. Applying SD clearly improves the spatial correlation of the downscaled rainfall pattern. This result is not consistent with that of Vrac et al. (2012). This can have several plausible causes. A first explanation is that the large-scale forcing in Vrac et al. (2012) is provided by ERA-40 reanalysis which has a horizontal resolution of 1.125° compared to 0.75° of ERA-I. So the local weather stations were located in at most 2–3 grid points of ERA-40 reanalysis. The use of DD at 50 km resolution thus improves the representation of fine scale structure of the atmospheric circulation. A second explanation is the use of local weather stations which retain the full spatial variability of the atmospheric circulation. Conversely, the use of gridded data such as ECA&D smoothes in part the horizontal variability after data interpolation explaining the weak sensitivity of the horizontal resolution in term of spatial correlation.

4.2 Temporal variability

Figure 9 displays the Taylor diagrams for the time series of the spatially average rainfall with respect to ECA&D, for the five sub-regions shown in Fig. 1. The standard deviation of the downscaled temperature is very close to that of ECA&D and the temporal correlation is never below 0.9.

Fig. 7 a Relative difference between the DD and observed 50th quantiles (1st and 3rd column from left) and 95th quantiles (2nd and 4th column from left) for rainfall in winter (1st and 2nd column from left) and summer (3rd and 4th column from left) over 1999–2008 (evaluation period) for ERA-I reanalysis (1st row), WRF/RUC 50 simulation (2nd row), WRF/DIF 50 simulation (3rd row), WRF/RUC 20 simulation (4th row) and WRF/DIF 20 simulation (5th row) **b** as in a but for SD

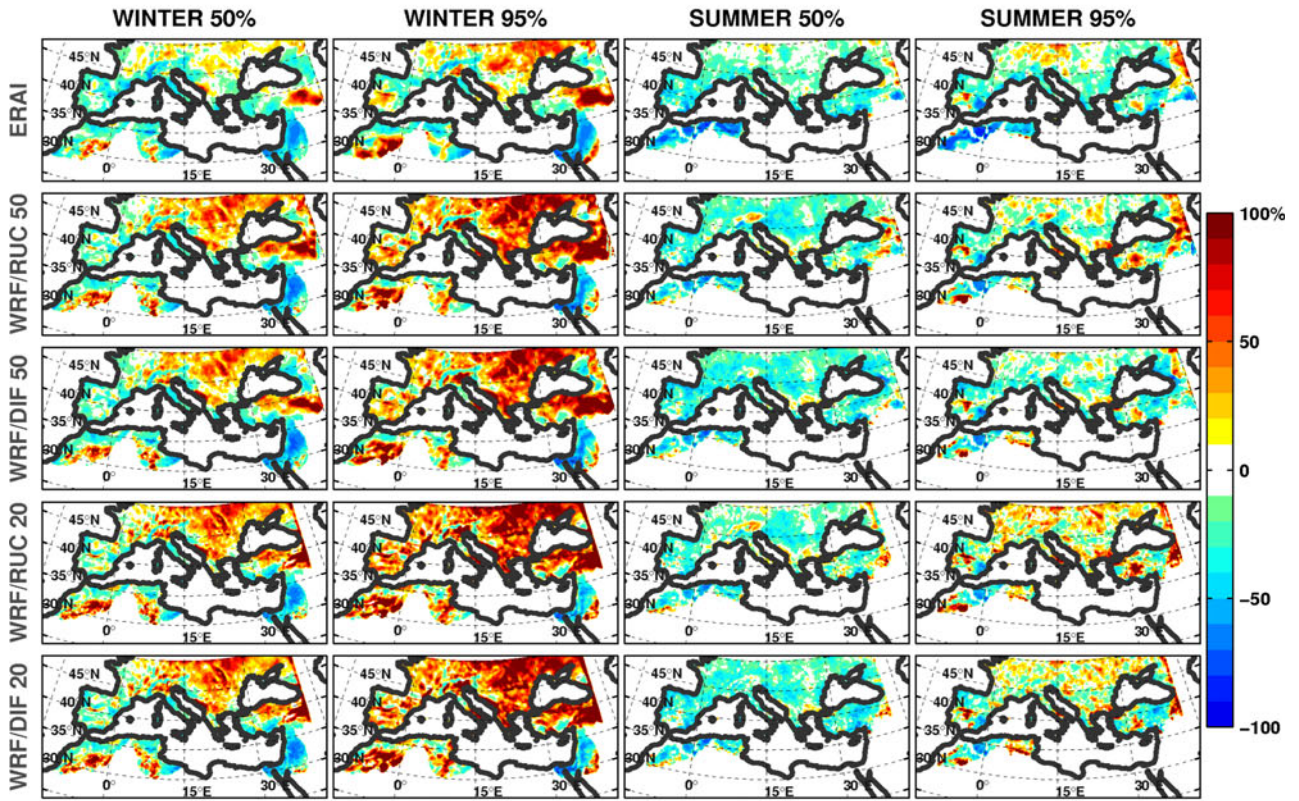
A very interesting feature is that the blue and red markers which have the same shape (circle, diamond, cross, star) are aligned on the radii of the circle which correspond to equal correlation. This means that applying SD to DD affects the standard deviation of the downscaled temperature but has no effect on the temporal correlation. This highlights the fact that the temperature downscaled with SD follows exactly the time evolution of the large-scale driving field used as input of SD. Regarding precipitation, the above discussion and conclusion stands. However, the temporal correlation of precipitation is much lower than of temperature. It can be as low as 0.2 in arid regions. It can reach 0.6–0.8 in mid-latitude regions. Therefore, Figs. 4, 5, 7 and 9 suggest that CDF-t is an efficient SD tool for bias correction but it retains the same intra-seasonal variability as the forcing data (i.e. ERA-I reanalysis or WRF simulations).

5 Discussion and conclusion

This study evaluates how SD, DD and SD/DD combined approach perform in retrieving the space–time variability of near-surface temperature and rainfall, as well as their extremes, over the Mediterranean region. The DD model used in this study is the Weather Research and Forecasting (WRF) model with 4 different configurations (varying land-surface models and resolution). The SD tool is the Cumulative Distribution Function-transform (CDF-t). To achieve a spatially resolved downscaling over the Mediterranean basin, the ECA&D gridded dataset is used for SD calibration and evaluation of SD and DD models.

One major added-value of DD suggested in previous studies is the accurate simulation of the spatial variability of the near surface temperature and rainfall. Comparatively SD which is calibrated on grid point (e.g. on surface station location) should produce better local time series. Our results invalidate these suggestions which show a much better correlation with SD than with DD. This first suggests that at 20–50 km resolutions, the three-dimensional processes explicitly resolved with DD only weakly contributes to the local value of temperature and precipitation with respect to local one-dimensional processes. Calibration of SD at each individual grid point is thus sufficient to reproduce accurately the spatial pattern. A second explanation is the use of gridded data such as ECA&D which

(A) Dynamical Downscaling



(B) Statistical Downscaling

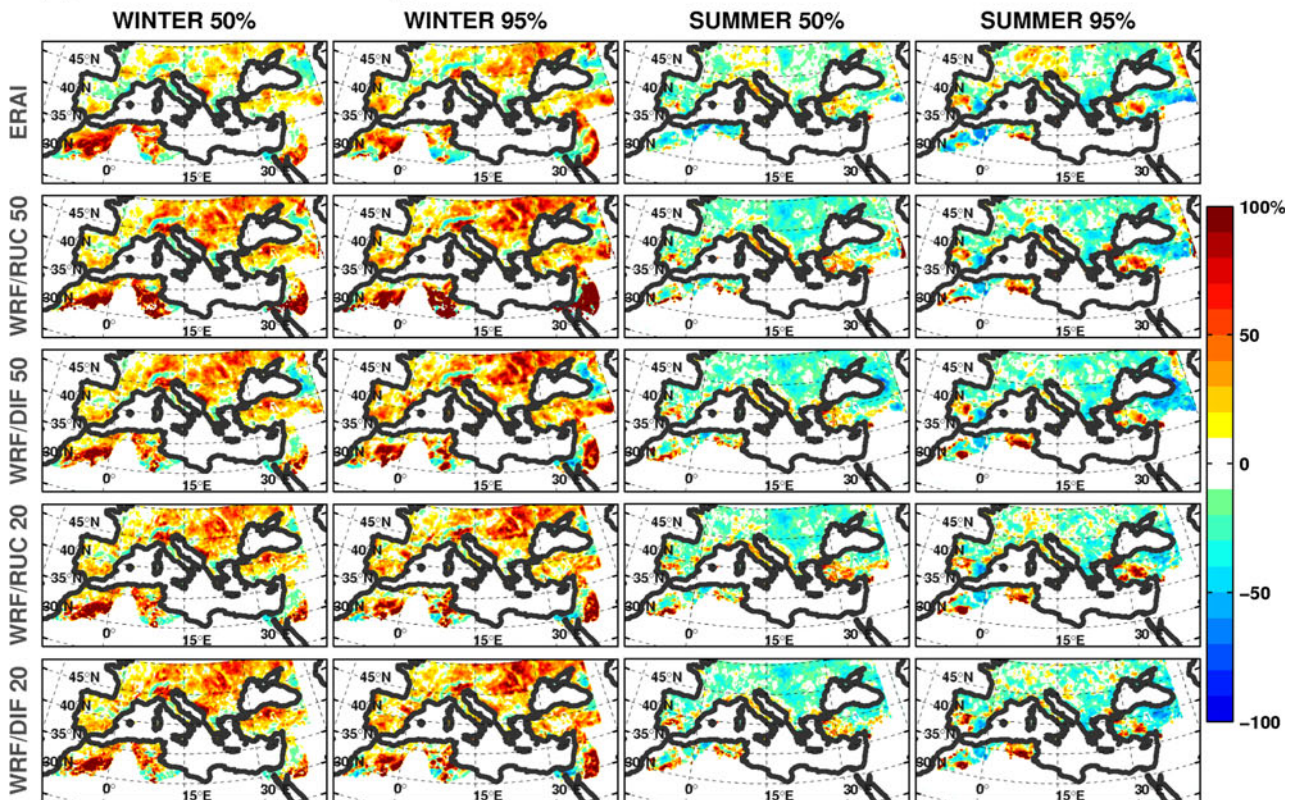
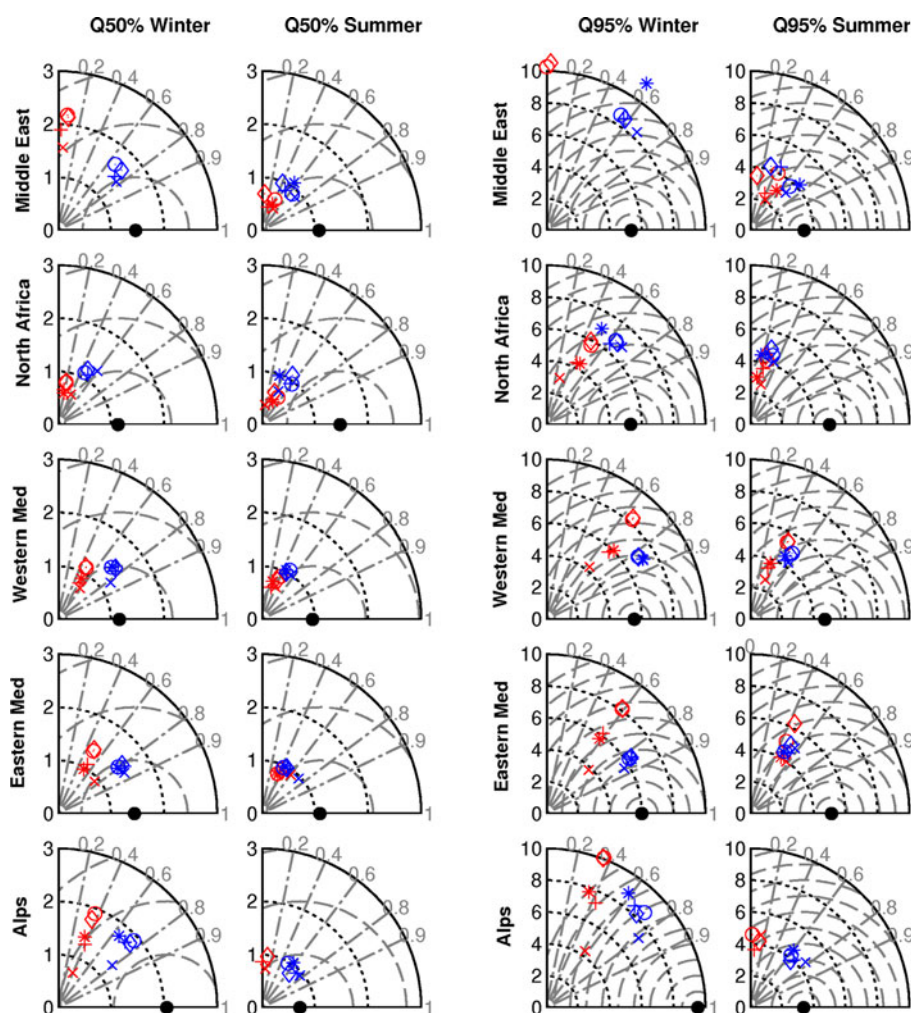


Fig. 8 Taylor diagrams for winter and summer rainfall median and extremes (q50obs and q95obs), for ERA-I, DD, SD and SD/DD, regards to ECA&D in the five sub-regions illustrated in Fig. 1. Root mean square differences in all figures are plotted with 1 mm of interval. Symbols in red stand for DD and ERA-I, while in blue for CDF-t. Black dot stands for the ECA&D, X for ERA-I; star for WRF/RUC50; circle for WRF/DIF50; cross for WRF/RUC20 and the diamond for WRF/DIF20



smoothes in part the horizontal variability after data interpolation and damps the added value of dynamical downscaling. This explains the weak sensitivity of the horizontal resolution in term of spatial correlation. It also explains partly the absence of added-value of the 2-stage downscaling approach which combines SD and DD in contradiction with Vrac et al. (2012) for instance. This highlights the limit of this inter-comparison which is tributary of the quality of the reference observations and the use of a gridded dataset. This point will be discussed hereafter. Regarding the absence of added-value of SD/DD combined approach, it can also have other origins. First, at 20 km resolution, WRF can produce local and less “predictable” atmospheric patterns which can increase the uncertainty when determining the mathematical function T. Second, the ERA-I re-analysis is already of “good quality” since it assimilates a large number of observations (some of which are also assimilated in ECA&D reanalysis). It makes the correction by CDF-t “easier” and thus more accurate, notably for temperature. Finally, the resolution of ERA-I is already fine (0.75°) and at most a factor 4 is applied with

WRF when a 20-km resolution is used, probably damping the expected added-value of DD.

Regarding, the temporal variability of SD, it is strongly driven by the temporal variability of its forcing. SD is thus efficient as a bias correction tool but does not show any added-value regarding the time variability of the downscaled field.

Regarding the quality of the reference observation dataset, Fig. 10 presents the Taylor diagrams for the time series of the temperature and rainfall from ERA-I and SD and DD models with respect to local measurements collected at three Mediterranean stations in the frame of HyMeX. The locations of these stations are shown in Fig. 1 and correspond to two coastal stations in Israel and France and one Italian station in the Alps, at an altitude of 1,700 meters. This figure shows that at these stations, ECA&D data (black dot) can be significantly different from the local measurements (red dot). As in Fig. 9, SD displays the same temporal correlation with respect to the observations as its forcing data (i.e. ERA-I reanalysis or WRF simulations). In most cases, the temporal correlation of the downscaled data

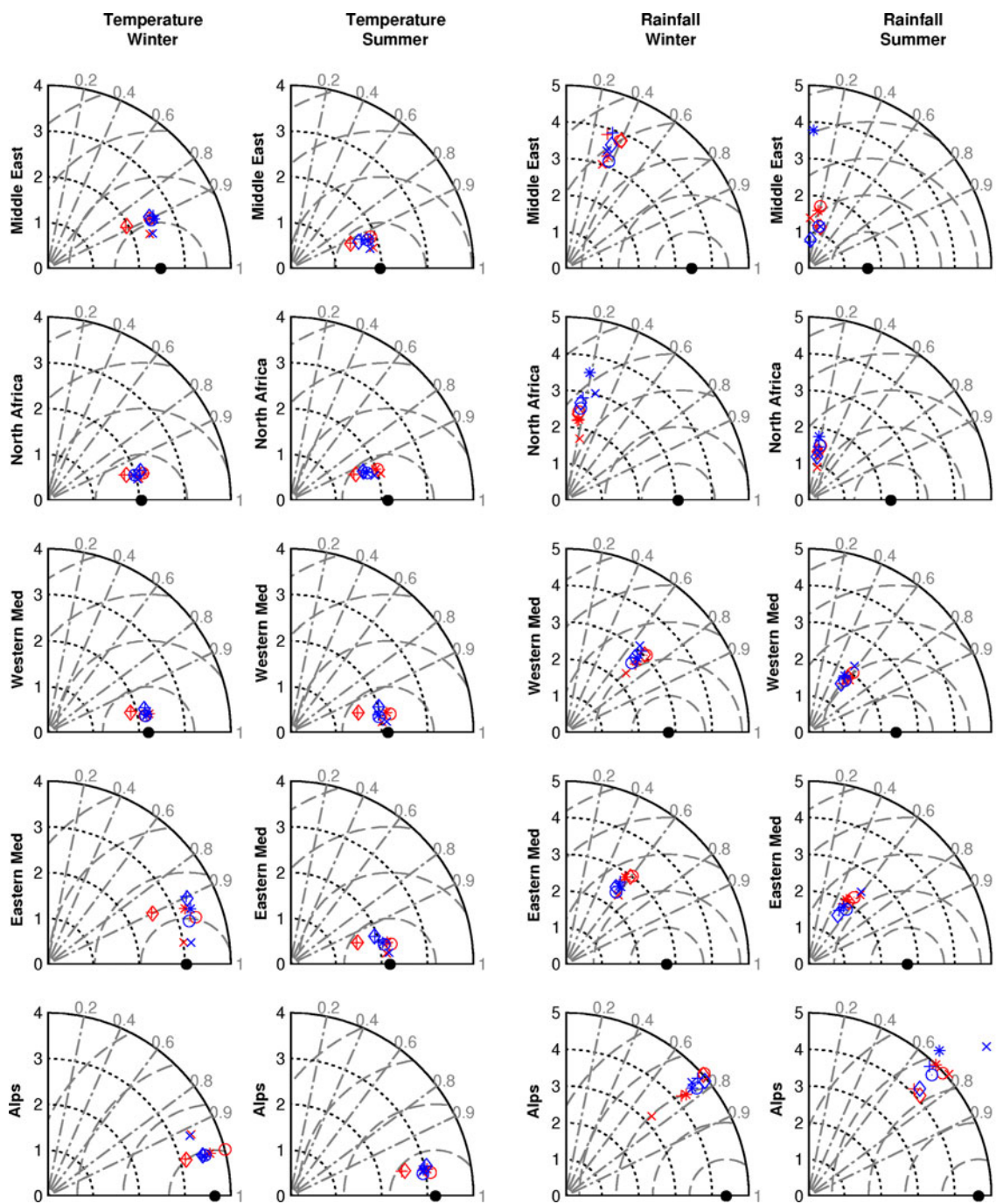


Fig. 9 Taylor diagrams for winter and summer temperature and rainfall, for ERA-I, DD, SD and SD/DD regards to ECA&D. Analyzed time series correspond to the spatial average of all grid points within the five sub-regions illustrated in Fig. 1. Root mean square differences in all figures are plotted with 1 mm and 1 °C of

interval. Symbols in red stand for DD and ERA-I, while in blue for CDF-t. Black dot stands for the ECA&D, X for ERA-I; star for WRF/RUC50; circle for WRF/DIF50; cross for WRF/RUC20 and the diamond for WRF/DIF20

with respect to the local observations is equal or larger than when ECA&D data is used as reference. This highlights the strong added-value of DD if it improves the temporal variability with respect to ERA-I. In terms of standard deviation, there is no systematic behavior. However, one can note that downscaled data with DD can be closer to the

local measurements than with SD, as illustrated for winter rainfall in Southern France and in the Italian Alps.

Finally, an issue that has been investigated but not detailed in the article is the local occurrence of different observed distributions between the calibration and evaluation periods, which does not exist in ERA-I or WRF. This

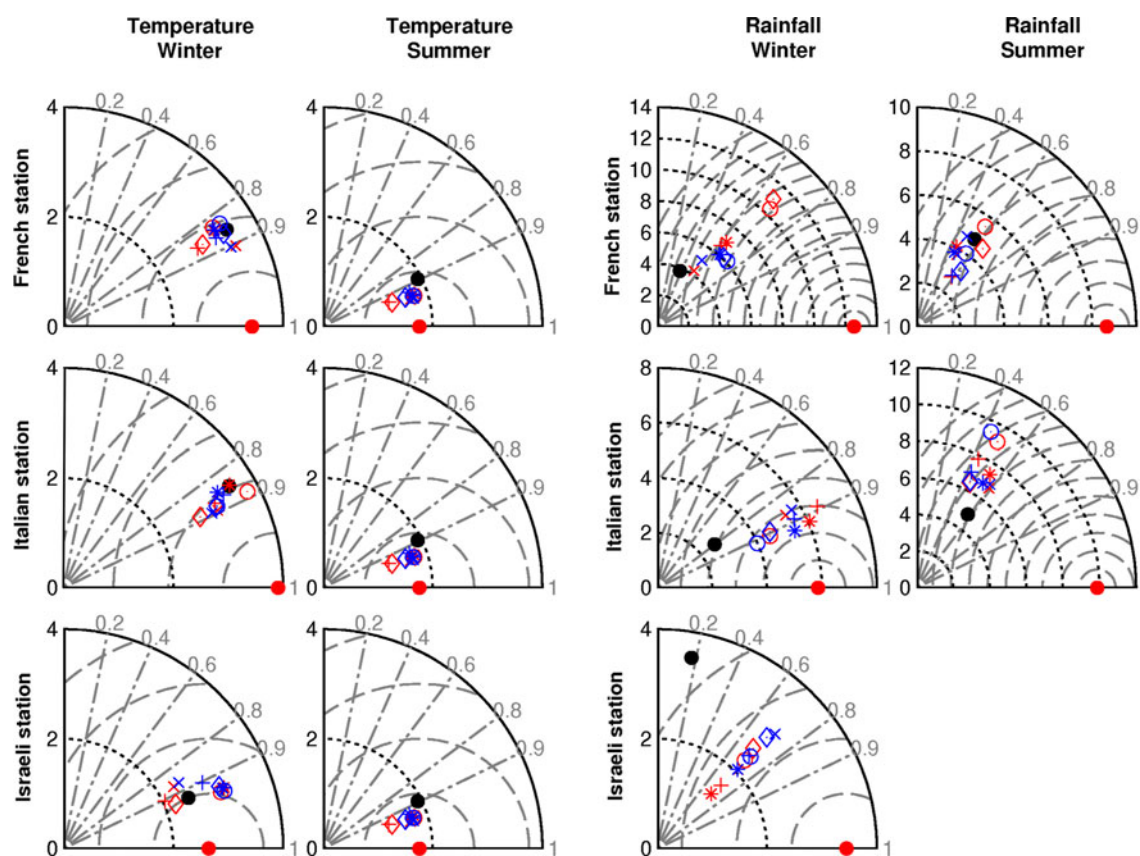


Fig. 10 Taylor diagrams for winter and summer temperature and rainfall for ERA-I, ECA&D, DD, SD and SD/DD regarding to three station observations for the period 2003–2008. All datasets are interpolated to the station locations, shown in Fig. 1. No rainfall has been reported to the Israeli station during the summer period. Root

mean square differences in all figures are plotted with 1 mm and 1 °C of interval. Symbols in red stand for DD and ERA-I, while in blue for CDF-t. Red dot stands for the station observations; black dot stands for the ECA&D, X for ERA-I; star for WRF/RUC50; circle for WRF/DIF50; cross for WRF/RUC20 and the diamond for WRF/DIF20

can be due to a modification of the instrumentation system, a change in the close by environment of the meteorological sensor, etc. Kolmogorov–Smirnov tests have been performed to check these outliers and they appeared marginal, even though they might impact on evaluation of the temperature and rainfall distributions locally.

This study demonstrates the added value of a multi-techniques and multi configurations approach for the assessment of SD and DD uncertainties, the identification of the limits and advantages of the downscaling techniques and a better understanding of the regional climate. It also highlighted the strong sensitivity of DD with WRF with respect to the choice of the physical parameterization. Much work has already investigated to sensitivity of simulated rainfall with regards to WRF parameterizations but over other regions (Flaounas et al. 2010; Cr  tat et al. 2012). Future work will investigate the sensitivity to physical parameterizations of temperature and rainfall simulated with WRF over the Mediterranean basin. It is in part a first natural step to quantify uncertainties before performing regional climate downscaling of CMIP5 simulations run in

anthropogenic scenarios. However, this assessment does not ensure that their performance will be similar, better or worse when projected in future climate for similar or specific reasons. Among the similar causes, the evolution of land use can affect locally the regional climate and its modeling with both SD and DD. If the large-scale forcing evolves the SD empirical relationship may fail because of the lack of similar situations in the recent climate. However, besides these inherent limitations which are difficult to anticipate, a natural follow-up of this study is the application of SD and DD to CMIP5 climate simulations in the frame of MED-CORDEX and HyMeX. A first evaluation of DD of CMIP5 historical runs has been performed to evaluate the ability of DD to reproduce the variability of the Mediterranean cyclones (Flaounas et al. 2012b). Future work will aim at applying SD and DD to CMIP5 simulations in anthropogenic scenarios.

Acknowledgments We are thankful to the two anonymous referees who helped to improve the manuscript significantly. We are grateful to Efrat Morin and the Israeli meteorological service for providing the Israeli stations measurements, to Guy Delrieu for providing

observations from the French meteorological stations and to the Ev-K2-CNR Committee which provided measurements from the Italian stations, collected within the SHARE project thanks to contributions from the Italian National Research Council and the Italian Ministry of Foreign Affairs. This research has received funding from ANR MEDUP and McSIM and GIS “Climat-Environnement-Société” MORCE-MED projects and from HyMeX program through INSU MISTRALS support. The WRF simulations have been performed at the GENCI (IDRIS) and IPSL computing centers.

References

- Beniston M, Stephenson DB, Christensen OB, Ferro CAT, Frei C, Goyette S, Halsnaes K, Holt T, Jylhä K, Koffi B, Palutikof J, Schöll R, Semmler T, Woth K (2007) Future extreme events in European climate: an exploration of regional climate model projections. *Clim Change* 81:71–95
- Boé J, Terray L (2008) A weather-type approach to analyzing winter precipitation in France: twentieth-century trends and the role of anthropogenic forcing. *J Clim* 21:3118
- Brussolo E, von Hardenberg J, Rebora N (2009) Stochastic versus dynamical downscaling of ensemble precipitation forecasts. *J Hydrometeorol* 10:1051–1061
- Bussotti F, Ferretti M (1998) Air pollution, forest condition and forest decline in southern Europe: an overview. *Environ Pollut* 101:49–65
- Busuoioc A, Tomozeiu R, Cacciamani C (2008) Statistical downscaling model based on canonical correlation analysis for winter extreme precipitation events in the Emilia-Romania region. *Int J Clim* 28:449–464
- Buzzi A, D’Isidoro M, Davolio S (2003) A case study of an orographic cyclone south of the Alps during the MAP SOP. *Q J R Meteorol Soc* 129:1795–1818
- Cannon AJ, Whitfield PH (2002) Downscaling recent streamflow conditions in British Columbia, Canada using ensemble neural network models. *J Hydrol* 259:136–151
- Carreau J, Vrac M (2011) Stochastic downscaling of precipitation with neural networks conditional mixture models. *Water Resour Res* (in revision)
- Claud C, Alhammoud B, Funatsu BM, Lebeaupin-Brossier C, Chaboureaud JP, Beranger K, Drobinski P (2012) A high resolution climatology of precipitation and deep convection over the Mediterranean region from operational satellite microwave data: development and application to the evaluation of model uncertainties. *Nat Hazards Earth Syst Sci* 12:785–798
- Crétat J, Pohl B, Richard Y, Drobinski P (2012) Uncertainties in simulating regional climate of Southern Africa: sensitivity to physical parameterizations using WRF. *Clim Dyn* 38:613–634
- Déqué M, Somot S (2008) Extreme precipitation and high resolution with ALADIN. *Idjaras Q J Hungarian Meteorol Serv* 112:179–190
- Dee D, Uppala S (2009) Variational bias correction of satellite radiance data in the ERA-Interim reanalysis. *Q J R Meteorol Soc* 135:1830–1841
- Drobinski P, Flamant C, Dusek J, Flamant PH, Pelon J (2001) Observational evidence and modeling of an internal hydraulic jump at the atmospheric boundary layer top during a tramontane event. *Bound Layer Meteorol* 98:497–515
- Drobinski P, Bastin S, Guénard V, Caccia JL, Dabas AM, Delville P, Protat A, Reitebuch O, Werner C (2005) Summer mistral at the exit of the Rhône valley. *Q J R Meteorol Soc* 131:353–375
- Drobinski P, Ducrocq V, Lionello P, the HyMeX ISSC, (2009a) HyMeX, a potential new CEOP RHP in the Mediterranean basin. *GEWEX Newslett* 19:5–6
- Drobinski P, Béranger K, Ducrocq V, Allen JT, Chronis G, Font J, Madec G, Papathanassiou E, Pinardi N, Sammari C, Taupier-Letage I (2009b) The HyMeX (Hydrological cycle in the Mediterranean experiment) program: the specific context of oceanography. *MERCATOR Newslett* 32:3–4
- Drobinski P, Ducrocq V, Lionello P (2010) Studying the hydrological cycle in the Mediterranean. *EOS Trans Am Geophys Union* 91:373
- Drobinski P, Ducrocq V, Lionello P, Homar V (2011) HyMeX, the newest GEWEX regional hydroclimate project. *GEWEX Newslett* 21:10–11
- Drobinski P, Anav A, Lebeaupin Brossier C, Samson G, Stéfanon M, Bastin S, Baklouti M, Béranger K, Beuvier J, Bourdallé-Badie R, Coquart L, D’Andrea F, De Noblet-Ducoudré N, Diaz F, Dutay JC, Ethe C, Foujols MA, Khvorostyanov D, Madec G, Mancip M, Masson S, Menut L, Palmieri J, Polcher J, Turquety S, Valcke S, Viovy N (2012) Modelling the regional coupled earth system (MORCE): application to process and climate studies in vulnerable regions. *Environ Model Softw* 35:1–18
- Ducrocq V, Nuissier O, Ricard D, Lebeaupin C, Thouvenin T (2008) A numerical study of three catastrophic precipitating events over Western Mediterranean region (Southern France). Part II: mesoscale triggering and stationarity factors. *Q J R Meteorol Soc* 134:131–145
- Dudhia J (1989) Numerical study of convection observed during the winter monsoon experiment using a mesoscale two dimensional model. *J Atmos Sci* 46:3077–3107
- Fischer PH, Brunekreef B, Lebreton E (2004) Air pollution related deaths during the 2003 heat wave in the Netherlands. *Atmos Environ* 38:1083–1085
- Flaounas E, Bastin S, Janicot S (2010) Regional climate modelling of the 2006 West African monsoon: sensitivity to convection and planetary boundary layer parameterisation using WRF. *Clim Dyn* 36:1083–1105
- Flaounas E, Drobinski P, Borga M, Calvet JC, Delrieu G, Morin E, Tartari G, Toffolon R (2012a) Assessment of gridded observations used for climate model validation in the Mediterranean region: the HyMeX and MED-CORDEX framework. *Environ Res Lett* 7:024017. doi:10.1088/1748-9326/7/2/024017
- Flaounas E, Drobinski P, Bastin S (2012b) Dynamical downscaling of IPSL-CM5 CMIP5 historical simulations over the Mediterranean: benefits on the representation of regional surface winds and cyclogenesis. *Clim Dyn* (under revision)
- Frei C, Christensen JH, Déqué M, Jacob D, Jones RG, Vidale PL (2003) Daily precipitation statistics in regional climate models: evaluation and intercomparison for the European Alps. *J Geophys Res* 108(D3):4124. doi:10.1029/2002JD002287
- Frei C, Schöll R, Fukutome S, Schmidli J, Vidale PL (2006) Future change of precipitation extremes in Europe: intercomparison of scenarios from regional climate models. *J Geophys Res* 111:D06105. doi:10.1029/2005JD005965
- García-Herrera R, Diaz J, Trigo RM, Hernández E (2005) Extreme summer temperatures in Iberia: health impacts and associated synoptic conditions. *Ann Geophys* 23:239–251
- Ghosh S, Mujumdar PP (2008) Statistical downscaling of GCM simulations to streamflow using relevance vector machine. *Adv Water Resour* 31:132–146
- Giorgi F (2006) Climate change hot-spots. *Geophys Res Lett* 33:L08707. doi:10.1029/2006GL025734
- Giorgi F, Lionello P (2007) Climate change projections for the Mediterranean region. *Global Planet Change*. doi:10.1016/j.gloplacha.2007.09.005
- Giorgi F, Coln J, Ghassem A (2009) Addressing climate information needs at the regional level. The CORDEX framework. *WMO Bull* (July 2009 issue)

- Goubanova K, Echevin V, Dewitte B, Codron F, Takahashi K, Terray P, Vrac M (2010) Statistical downscaling of sea-surface wind over the Peru-Chile upwelling region: diagnosing the impact of climate change from the IPSL-CM4 model. *Clim Dyn* 36:1365–1378
- Guénard V, Drobinski P, Caccia JL, Campistron B, Bénech B (2005) An observational study of the mesoscale mistral dynamics. *Bound Layer Meteorol* 115:263–288
- Harpham C, Wilby RL (2005) Multi-site downscaling of heavy daily precipitation occurrence and amounts. *J Hydrol* 312(2005): 235–255
- Haylock MR, Hofstra N, Klein Tank AMG, Klok EJ, Jones PD, New M (2008) A European daily high-resolution gridded dataset of surface temperature and precipitation. *J Geophys Res* 113:D20119. doi:10.1029/2008JD10201
- Herrmann M, Somot S, Calmanti S, Dubois C, Sevault F (2011) Representation of spatial and temporal variability of daily wind speed and of intense wind events over the Mediterranean Sea using dynamical downscaling: impact of the regional climate model configuration. *Nat Hazards Earth Syst Sci* 11:1983–2001
- Hong SY, Pan HL (1996) Non-local boundary layer vertical diffusion in medium-range forecast model. *Mon Weather Rev* 124:1215–1238
- Hong SY, Juang HMH, Zhao Q (1998) Implementation of prognostic cloud scheme for a regional spectral model. *Mon Weather Rev* 126:2621–2639
- Hong SY, Dudhia J, Chen SH (2004) A revised approach to ice microphysical processes for the bulk parameterization of clouds and precipitation. *Mon Weather Rev* 132:103–120
- Huth R (2002) Statistical downscaling of daily temperature in central Europe. *J Clim* 15:1731–1742
- Kain JS (2004) The Kain–Fritsch convective parameterization: an update. *J Appl Meteorol* 43:170–181
- Klein Tank AMG et al (2002) Daily dataset of 20th-century surface air temperature and precipitation series for the European Climate Assessment. *Int J Climatol* 22:1441–1453
- Klemp JB, Skamarock WC, Dudhia J (2007) Conservative split-explicit time integration methods for the compressible nonhydrostatic equations. *Mon Weather Rev* 135:2897–10519
- Köppen W (1936) Das geographische system der Klimate. In: Köppen W, Geiger G (eds) *Handbuch der Klimatologie*, vol 1, C. Gebr. Borntraeger, pp 1–44
- Lagouvardos K, Kotroni V (2000) Use of METEOSAT water-vapour images for the diagnosis of a vigorous stratospheric intrusion over Central Mediterranean. *Meteorol Appl* 7:205–210
- Lavaysse C, Vrac M, Drobinski M, Lengaigne M, Vischel T (2012) Statistical downscaling of the French Mediterranean climate: assessment for present and projection in an anthropogenic scenario. *Nat Hazards Earth Syst Sci* 12:651–670
- Lebeaupin Brossier C, Béranger K, Deltel C, Drobinski P (2011) The Mediterranean response to different space-time resolution atmospheric forcings using perpetual mode sensitivity simulations. *Ocean Model* 36:1–25
- Lebeaupin Brossier C, Béranger K, Drobinski P (2012a) Sensitivity of the North-Western Mediterranean coastal and thermohaline circulations as simulated by the 1/12° resolution oceanic model NEMO-MED12 to the space-time resolution of the atmospheric forcing. *Ocean Model* 43–44:94–107
- Lebeaupin Brossier C, Béranger K, Drobinski P (2012b) Ocean response to strong precipitation events in the Gulf of Lions (North-Western Mediterranean Sea): a sensitivity study. *Ocean Dyn* 62:213–226
- Lebeaupin Brossier C, Drobinski P, Béranger K, Bastin S, Orain F (2012c) Ocean memory effect on the dynamics of coastal heavy precipitation preceded by a mistral event in the North-Western Mediterranean. *Q J R Meteorol Soc* (in revision)
- Lebeaupin C, Ducrocq V, Giordani H (2006) Sensitivity of Mediterranean torrential rain events to the sea surface temperature based on high-resolution numerical forecasts. *J Geophys Res* 111: D12110. doi:10.1029/2005JD006541
- Llasat-Botija M, Llasat MC, López L (2007) Natural hazards and the press in the Western Mediterranean region. *Adv Geosci* 12: 81–85
- Lo JCF, Yang ZL, Pielke RA Sr (2008) Assessment of three dynamical climate downscaling methods using the weather research and forecasting (WRF) model. *J Geophys Res* 113:D09112. doi:10.1029/2007JD009216
- Mass FC, Ovens D, Westrick K, Colle BA (2002) Does increasing horizontal resolution produce more skillful forecast? *Bull Am Meteorol Soc* 83:407–430
- Michelangioli PA, Vrac M, Loukos H (2009) Probabilistic downscaling approaches: application to wind cumulative distribution functions. *Geophys Res Lett*. doi:10.1029/2009GL038401
- Mitchell TD, Jones PD (2005) An improved method of constructing a database of monthly climate observations and associated high-resolution grids. *Int J Climatol* 25:693–712
- Mlawer EJ, Taubman SJ, Brown PD, Iacono MJ, Clough SA (1997) Radiative transfer for inhomogeneous atmosphere: RRTM, a validated correlated-k model for the longwave. *J Geophys Res* 102(D14):16663–16682
- Noh Y, Cheon WG, Hong SY, Raasch S (2003) Improvement of the k-profile model for the planetary boundary layer based on large eddy simulation data. *Bound Layer Meteorol* 107:401–427
- Oettli P, Sultan B, Baron C, Vrac M (2011) Are regional climate models relevant for crop yield prediction in West Africa? *Environ Res Lett* 6. doi:10.1088/1748-9326/6/1/014008
- Omrani H, Drobinski P, Dubos T (2012) Optimal nudging strategies in regional climate modelling: investigation in a big-brother experiment over the European and Mediterranean regions. *Clim Dyn* (submitted)
- Pace G, Di Sarra A, Meloni D, Piacento S, Chamard P (2005) Aerosol optical properties at Lampedusa (Central Mediterranean). 1. Influence of transport and identification of different aerosol types. *Atmos Chem Phys Disc* 5:4929–4969
- Patterson S (1956) *Weather Analysis and Forecasting*. McGraw-Hill, New York 428 p
- Piani C, Haerter JO, Coppola E (2010) Statistical bias correction for daily precipitation in regional climate models over Europe. *Theor Appl Climatol* 99:187–192
- Quintana Seguí P, Ribes A, Martin E, Habets F, Boé J (2010) Comparison of three downscaling methods in simulating the impact of climate change on the hydrology of Mediterranean basins. *J Hydrol* 383:111–124
- Raymond D, Wilkening M (1980) Mountain-induced convection under fair weather conditions. *J Atmos Sci* 37:2693–2706
- Romero R, Doswell CA III, Ramis C (2000) Mesoscale numerical study of two cases of long-lived quasistationary convective systems over eastern Spain. *Mon Weather Rev* 128:3731–3751
- Ruti PM, Marullo S, D’Ortenzio F, Tremant M (2008) Comparison of analyzed and measured wind speeds in the perspective of oceanic simulations over the Mediterranean basin: analyses, QuikSCAT and buoy data. *J Mar Syst* 70:33–48
- Ruti P, Somot S, Dubois C, Calmanti S, Ahrens B, Aznar R, Bartholy J, Béranger K, Bastin S, Brauch J, Calvet JC, Carillo A, Alias A, Decharme B, Dell’Aquila A, Djurdjevic V, Drobinski P, Elizalde Arellano A, Gaertner M, Galan P, Gallardo C, Giorgi F, Gualdi S, Bellucci A, Harzallah A, Herrmann M, Jacob D, Khodayar S, Krichak S, Lebeaupin C, Lheveder B, Li L, Liguori G, Lionello P, Baris O, Rajkovic B, Sevault F, Sannino G (2012) MED-CORDEX initiative for Mediterranean climate studies. *Bull Am Meteorol Soc* (submitted)

- Sailor DJ, Xiangshang L (1999) A semi-empirical downscaling approach for predicting regional temperature impacts associated with climatic change. *J Clim* 12:103–114
- Salameh T, Drobinski P, Vrac M, Naveau P (2009) Statistical downscaling of near-surface wind over complex terrain in southern France. *Meteorol Atmos Phys* 103:243–256
- Salameh T, Drobinski P, Dubos T (2010) The effect of indiscriminate nudging time on large and small scales in regional climate modelling: application to the Mediterranean basin. *Q J R Meteorol Soc* 136:170–182
- Schmidli J, Frei C, Vidale PL (2006) Downscaling from GCM precipitation: a benchmark for dynamical and statistical downscaling methods. *Int J Climatol* 26(5):679–689
- Schmidli J, Goodess CM, Frei C, Haylock MR, Hundecha Y, Ribalaygua J, Schmith T (2007) Statistical and dynamical downscaling of precipitation: An evaluation and comparison of scenarios for the European Alps. *J Geophys Res* 112:D04105. doi:[10.1029/2005JD007026](https://doi.org/10.1029/2005JD007026)
- Semenov MA, Barrow EM (1997) Use of a stochastic weather generator in the development of climate change scenarios. *Clim Res* 35:397–414
- Skamarock WC, Klemp JB (2008) A time-split nonhydrostatic atmospheric model for weather research and forecasting applications. *J Comput Phys* 227:3465–3485
- Skamarock WC, Klemp JB, Dudhia J, Gill DO, Barker DM, Dudhia J, Huang X, Wang W, Powers Y (2008) A description of the advanced research WRF Ver.30. NCAR technical note. NCAR/TN-475 + STR. Mesoscale and Microscale Meteorology Division, National Centre for Atmospheric Research, Boulder Colorado, USA, p 113
- Smirnova TG, Brown JM, Benjamin SG (1997) Performance of different soil model configurations in simulating ground surface temperature and surface fluxes. *Mon Weather Rev* 125:1870–1884
- Sotillo M, Ratsimandresy AW, Carretero J, Bentamy A, Valero F, Gonzalez-Rouco F (2005) A high resolution 44-year atmospheric hindcast for the Mediterranean Basin: contribution to the regional improvement of global reanalysis. *Clim Dyn* 25:219–236
- Spak S, Holloway T, Lynn B, Goldberg R (2007) A comparison of statistical and dynamical downscaling for surface temperature in North America. *J Geophys Res* 112:D08101. doi:[10.1029/2005JD006712](https://doi.org/10.1029/2005JD006712)
- Stohl A, Spichtinger-Rakowsky N, Bonasoni P, Feldmann H, Memmesheimer M, Scheel HE, Trickl T, Hubener S, Ringer W, Mandl M (2000) The influence of stratospheric intrusions on alpine ozone concentrations. *Atmos Environ* 34:1323–1354
- Trigo Isabel F, Bigg GR, Davies TD (1999) Climatology of cyclogenesis mechanisms in the Mediterranean. *Mon Weather Rev* 130:549–569
- Uppala S, Dee D, Kobayashi S, Berrisford P, Simmons A (2008) Towards a climate data assimilation system: status update of ERA-interim. *ECMWF Newsl* 115:12–18
- Vautard R, Yiou P, D'Andrea F, de Noblet N, Viovy N, Cassou C, Polcher J, Ciais P, Kageyama M, Fan Y (2007) Summertime European heat and drought waves induced by wintertime Mediterranean rainfall deficit. *Geophys Res Lett* 34:L07711. doi:[10.1029/2006GL028001](https://doi.org/10.1029/2006GL028001)
- Vrac M, Naveau P (2007) Stochastic downscaling of precipitation: from dry events to heavy rainfalls. *Water Resour Res* 43:W07402. doi:[10.1029/2006WR005308](https://doi.org/10.1029/2006WR005308)
- Vrac M, Hayhoe K, Stein M (2007a) Identification and inter-model comparison of seasonal circulation patterns over North America. *Int J Clim* 27:603–620
- Vrac M, Marbaix P, Paillard D, Naveau P (2007b) Non-linear statistical downscaling of present and LGM precipitation and temperatures over Europe. *Clim Past* 3:669–682
- Vrac M, Stein M, Hayhoe K (2007c) Statistical downscaling of precipitation through nonhomogeneous stochastic weather typing. *Clim Res* 34:169–184
- Vrac M, Naveau P, Drobinski P (2007d) Modeling pairwise dependences in precipitation intensities. *Nonlin Process Geophys* 14:789–797
- Vrac M, Drobinski P, Merlo A, Herrmann M, Lavaysse C, Li L, Somot S (2012) Dynamical and statistical downscaling of the French Mediterranean climate: uncertainty assessment. *Nat Hazards Earth Syst Sci* (in press)
- Weissmann M, Braun FJ, Gantner L, Mayr GJ, Rahm S, Reitebuch O (2005) The alpine mountain–plain circulation: airborne Doppler lidar measurements and numerical simulations. *Mon Weather Rev* 133:3095–3109
- Wilby RL, Dawson CW, Barrow EM (2002) SDSM—a decision support tool for the assessment of regional climate change impacts. *Environ Model Softw* 17:145–157
- Wilks DS, Wilby RL (1999) The weather generation game: a review of stochastic weather models. *Prog Phys Geogr* 23:329–357
- Yang C, Chandler RE, Isham VS (2005) Spatial-temporal rainfall simulation using generalized linear models. *Water Resour Res* 41:W11415. doi:[10.1029/2004WR003739](https://doi.org/10.1029/2004WR003739)
- Zanis P et al (2003) Forecast, observation and modelling of a deep stratospheric intrusion event over Europe. *Atmos Chem Phys* 3:763–777